Synthesis and characterisation of a mussel-inspired hydrogel film coating for biosensors

Jonathan M. Millican[1], Eva Bittrich[2], Anja Caspari[2], Kathrin Pöschel[2], Astrid Drechsler[2], Uwe Freudenberg[2], Timothy G. Ryan[3], Richard. L. Thompson[1], Doris Pospiech[2], Lian R. Hutchings[1]*

1. Department of Chemistry, Durham University, Durham, DH1 3LE, UK
2. Leibniz-Institut für Polymerforschung e.V., Dresden, Germany
3. Epigem Ltd., Redcar, UK

*l.r.hutchings@durham.ac.uk

Abstract

Mussel-inspired, catechol-containing monomers are being increasingly utilised to design versatile, adhesive, functional copolymers. This work reports the synthesis and detailed characterisation of a novel terpolymer comprising dopamine methacrylamide (DMA), in order to produce surface coatings capable of acting as biosensors for, e.g., toxins. DMA is copolymerised with 2-hydroxyethyl methacrylate (HEMA) and glycidyl methacrylate (GMA) using free radical polymerisation. The copolymers are subsequently deposited as a thin film using spin-coating. It is demonstrated that a terpolymer comprising HEMA, GMA and DMA can immobilise an IgG antibody on the film surface. The terpolymer therefore has the potential to be used as a coating in biosensing devices. It is also demonstrated that the presence of DMA impacts the copolymer properties. *In-situ* ellipsometry is used to confirm the important role of the catechol group on copolymer adhesion and significant desorption was observed in the absence of DMA.

Introduction

Aflatoxins are hepatotoxic compounds produced by the fungus *Aspergillus*. Aflatoxin M1 is an animal metabolite of aflatoxin B1 which can be excreted into milk and is extremely carcinogenic to humans.[1] The presence of aflatoxin M1 in dairy products is of concern to human health and a maximum permissible level of 50 ng L^{-1} is mandated by the European Commission.[2] Existing methods of detection for aflatoxins include the use of high performance liquid chromatography, surface plasmon resonance or mass spectrometry, however there is increasing need for low cost, portable devices with sufficient sensitivity to detect aflatoxins.[1, 3-5] A common method for diagnosis or detection of an analyte in biomedical science is to use an array of antibodies, e.g. in an enzyme-linked immunosorbent assay (ELISA), in which a surface-bound antigen can be detected.[6] An alternative approach is to immobilise antibodies on a surface and pass the analyte directly over the array. Such a device would require facile and versatile antibody immobilisation.

Biomolecule immobilisation can be facilitated using bio-inspired surface coatings. A common example of such an approach is the use of the catechol functional group (*e.g.* in dopamine), inspired by the adhesion mechanism of mussels.[7] Polydopamine coatings, first reported in 1997 by Messersmith *et al.*,[8] have been used to adhere to virtually any surface, which allows functionalisation of otherwise inert substrates, and for many other applications.[9]

Alternatively, chemical modification of dopamine provides a route to a more controlled inclusion of the catechol moiety into a material. Dopamine acrylamide (DA) or dopamine methacrylamide (DMA) can be used as monomers in radical copolymerisations, which introduce catechol functionalities into the polymer.[10, 11] These monomers have been shown to enhance the adhesion of polymers and materials with diverse functionalities have been developed for a variety of applications including antifouling, antibacterial and reversibly adhesive coatings.[10, 12, 13] In the absence of oxygen, DA and DMA can be copolymerised with a variety of vinyl comonomers with DA/DMA molar fractions of up to 50%. However, it has also been proposed that the catechol group has an impact during the polymerisation (on *e.g.* molecular weight, dispersity, crosslinking) and, in reactions comprising catechol-containing monomer molar fractions greater than 50%, radical scavenging prevents the synthesis of soluble polymers.[14, 15]

The current work presents the synthesis and characterisation of a novel functional adhesive statistical terpolymer, comprising DMA, hydroxyethyl methacrylate (HEMA), and glycidyl methacrylate (GMA). The target material was designed to adhere strongly to almost any device surface via the catechol functionality of the DMA, providing a coating capable of immobilising antibodies intended to detect aflatoxin M1 in a biomedical device. HEMA was selected to make the terpolymer hydrophilic (yet not water soluble) to prevent collapse of the terpolymer in aqueous (biological) environments. HEMA is a versatile monomer yielding biocompatible polymers, often copolymerised with cross-linkable monomers to form hydrogels for biomedical applications. Poly(HEMA) is hydrophilic, but considered insoluble in water due to the methacrylate backbone.[16] Poly(HEMA) also has anti-fouling properties, often utilised in biomedical applications, most notably in contact lenses.[17, 18] GMA was included in this work to facilitate the immobilisation of antibodies to the solution-coating interface and to further support attachment of the copolymer films to surfaces via the epoxide ring.[19, 20] Immobilisation of an antibody on the terpolymer coating is subsequently demonstrated to confirm the potential of the terpolymer coatings in biosensing applications.

Experimental

Materials

Dopamine hydrochloride (99%), sodium carbonate monohydrate (99.5%), sodium tetraborate (99.5%, borax), anhydrous magnesium sulfate (99.5%), and dimethyl sulfoxide-d_6 (99.9% D atom, DMSO-d6) were supplied by Sigma-Aldrich, UK, and used as received. Azobisisobutyronitrile (98%, AIBN) was supplied by Sigma-Aldrich, UK, and recrystallised from methanol before use. Methacrylic anhydride (94%), glycidyl methacrylate (97%, GMA) and

2-hydroxyethyl methacrylate (97%, HEMA) were supplied by Sigma-Aldrich, UK, and passed through a column of activated alumina before use to purify and to remove inhibitor. Hydrochloric acid (36.5% w/v solution) and *N,N*-dimethylformamide (anhydrous, 99.8%, DMF) were supplied by Fisher Scientific, UK, and used as received. Phosphate buffered saline (PBS) tablets, sodium phosphate monobasic (99%) and sodium phosphate dibasic (99%) were all obtained from Merck, Germany, and used as received. Anti-aflatoxin M1 antibody A16A-1 was supplied by AntiProt, Puchheim, Germany, stored at 4 °C and used within 4 weeks.

DMA synthesis

DMA was synthesised using the method of Messersmith and coworkers.[21] Full experimental details can be found in the supplementary information.

Polymer synthesis

Typical free radical copolymerisation of HEMA and DMA (HD-90/10)

The copolymerisation of HEMA (1.04 g, 8.00 mmol) and DMA (0.20 g, 0.89 mmol) was initiated using AIBN (15 mg, 0.09 mmol) in 12 mL of DMF in a 50 mL two-necked round-bottomed flask, fitted with a condenser and the other neck sealed with a rubber septum. The solution was sparged with nitrogen for 60 minutes and magnetically stirred. An initial sample was removed for analysis with a syringe. The flask was then heated to 70 °C in an oil bath under a nitrogen blanket. The reaction was allowed to proceed for 21 hours before a final sample was taken. The reaction solution was poured into diethyl ether, causing precipitation of white solid which was collected and dried overnight under vacuum. Yield = 1.16 g, 94%. M_n = 36200 g mol^{-1}, Đ = 3.17.^{1}H NMR (DMSO-d6, 400 MHz)δ (ppm) = 8.70 (s, 2H, Ph-O**H**), 6.61 – 6.41 (m, 3H, Ph-**H**), 4.80 (s, 1H, CH_2-O**H**), 4.11 (s, 1H, N**H**-CH_2), 3.88 (s, 2H, O-C**H$_2$**-CH_2), 3.55 (s, 2H, O-CH_2-C**H$_2$**), 3.33 (s, 2H, NH-C**H$_2$**), 3.15 (s), 2.90 (s), 2.77 (s), 1.80 (m, 6H, C-C**H$_3$**), 0.96, 0.77 (m, 3H, CH_2-C-C**H$_3$**,).

Free radical terpolymerisation of HEMA, GMA and DMA (HGD-80/10/10)

The terpolymerisation of HEMA (1.04 g, 8.00 mmol), GMA (0.14 g, 1.00 mmol) and DMA (0.22 g, 1.00 mmol) was initiated using AIBN (16 mg, 0.10 mmol) in 13 mL of DMF according to the procedure described above except that the reaction was allowed to proceed for 22.5 hours. A final sample was taken prior to precipitation of the polymer in diethyl ether. Yield = 0.97 g, 69%. M_n = 43400 g mol^{-1}, Đ = 3.23.^{1}H NMR (DMSO-d6, 400 MHz)δ (ppm):^{1}H NMR (DMSO-d6, 400 MHz)δ (ppm) = 8.69 (2s, 2H, Ph-O**H**), 6.65 – 6.44 (m, 3H, Ph-**H**), 4.81 (s, 1H, CH_2-O**H**), 4.62 (s, 1H, N**H**-CH_2), 4.26 (s, 1H, O-C**H$_2$**-CH *GMA*), 3.89 (s, 2H, O-C**H$_2$**-CH_2 *HEMA*), 3.73 (s, 1H, O-C**H$_2$**-CH *GMA*),3.59 (s, 2H, O-CH_2-C**H$_2$***HEMA*), 3.34 (s, 2H, NH-C**H$_2$**), 3.20, 2.90 (2s, 1H, O-CH-C**H$_2$** *GMA*), 2.66 (s, 2H, C**H$_2$**-Ph), 2.57 (s, 1H, O-CH-C**H$_2$** *GMA*), 2.12-1.75 (s, 2H, C**H$_2$**-C-CH_3), 0.96, 0.76 (m, 3H, CH_2-C-C**H$_3$**).

Free radical copolymerisation of HEMA and GMA (HG-90/10)

The copolymerisation of HEMA (1.56 g, 12.0 mmol) and GMA (0.19 g, 1.33 mmol) was initiated using AIBN (21 mg, 0.13 mmol) in 11 mL of DMF according to the procedure described above except for the following modifications. The reaction was allowed to proceed for 18.5 hours. A final sample was taken prior to precipitation of the polymer in diethyl ether. Yield = 1.32 g, 75%. M_n = 133500 g mol^{-1}, Đ = 4.26.^{1}H NMR (DMSO-d6, 400 MHz)δ (ppm) = 4.83 (s, 1H, CH_2-O**H**), 4.28 (s, 1H, O-C**H$_2$**-CH *GMA*), 3.91 (s, 2H, O-C**H$_2$**-CH_2*HEMA*), 3.72 (s, 1H, O-C**H$_2$**-CH *GMA*),3.61 (s, 2H, O-CH_2-C**H$_2$***HEMA*), 3.45 (s), 3.35 (s), 3.20, 2.87 (2s, 1H, O-CH-C**H$_2$** *GMA*), 2.73 – 1.80 (s, 2H, C**H$_2$**-C-CH_3), 0.96, 0.76 (m, 3H, CH_2-C-C**H$_3$**).

Monomer / Polymer Characterisation

Molecular weights were obtained by size exclusion chromatography (SEC) using a Viscotek TDA 302 with refractive index, viscosity, and light scattering detectors. 2 × 300 mm PLgel 5 µm mixed C-columns (Agilent, Stockport, UK, with a linear range of molecular weight from 200 to 2,000,000 g mol^{-1}) were used. Dimethylformamide (DMF) with 0.1 wt.% of lithium bromide was used as the eluent with a flow rate of 1.0 mL^{-1} at a temperature of 70 °C. Absolute molecular weights were obtained using data obtained by triple detection SEC with light scattering, using a *dn/dc* value of 0.076 mL g^{-1} for HEMA in DMF.[22]

^{1}H and ^{13}C NMR spectra were recorded on a Bruker-400 MHz spectrometer using DMSO-d_6 as a solvent. Spectra were referenced to the trace proton peaks present in DMSO-d_6 (2.50 ppm). NMR spectra were analysed using MestReNova (Mestrelab Research, Spain). DMF was used as an internal standard to calculate monomer conversion.

Substrate cleaning method

Silicon wafers were cleaned by immersion for 30 min in a flask containing 250 mL dichloromethane, before immersion for 30 minutes in 250 mL piranha solution (1:3 mixture of hydrogen peroxide and sulfuric acid), and then rinsed by immersion in 250 mL milliQ water. The cleaned wafers were stored for up to 24 hours in milliQ water before coating to prevent contamination, before being dried in a stream of nitrogen.

Spin-coating experiments

Copolymers were spin-coated onto substrates using either a POLOS 200 spin-coater or a Laurell WS-650MZ-23NPP spin-coater. Copolymers were dissolved in methanol at solution concentrations from 0.5% to 2% (w/v) and then passed through a 0.45 µm syringe filter. The cleaned silicon wafers were immobilised on the stage of the spin-coater using a vacuum pump and sufficient copolymer solution was applied to ensure the entire surface of the substrate was wetted. Spin speeds were varied between 1000 and 4000 rpm at acceleration rates of between 100 and 600 rpm s^{-1}. The parameters used for individual experiments are specified below. The spin duration was set to 75 s.

Atomic Force microscopy (AFM) experiments

AFM measurements were carried out in the peak force tapping mode by a Dimension FASTSCAN (Bruker-Nano, USA) using silicon nitride sensors FASTSCAN-C (Bruker, USA) with a nominal spring constant of 0.7 N/m and tip radius of 5 nm. The setpoint was 0.08 V.

Contact angle measurements

Specially prepared silicon wafers, laser-cut 20 mm x 20 mm squares with a 1 mm diameter central hole, were spin-coated as described above to obtain film thicknesses of around 150 nm (1000 rpm, 400 rpm s^{-1}, 2 wt% copolymer solution in methanol). The dynamic contact angles were determined using the Axisymmetric Drop Shape Analysis Profile (ADSA-P) captive bubble method with water as the contact fluid.[23] Each copolymer-coated wafer was immersed, face-down, in water and the copolymer coating was allowed to equilibrate for at least 30 minutes. Air was injected through the sample using a syringe pump connected to a needle, producing an air bubble trapped under the water-swollen copolymer film. The volume of the bubble was steadily increased for 60 s (advancing bubble contact angle), then the process was reversed (receding bubble contact angle). From the images of the bubble, the bubble radius (r), bubble volume (V) and bubble contact angle (θ_{bubble}) were calculated as function of time using drop profiles based on the Laplace equation. The liquid contact angle is then ($180° - \theta_{bubble}$). Advancing and receding contact angles were determined by averaging over time intervals with nearly constant contact angles while the bubble volume was decreased or increased, respectively.[24] For each polymer sample, three silicon wafers were spin-coated, and the bubble expansion/retraction cycle was repeated at least three times for each coated silicon wafer on three positions of the sample. Representative measurements are illustrated in Figure SI-1.

Streaming potential measurements

Streaming potential measurements were carried out to determine the zeta potential of the polymers using a SurPASS 3 (Anton Paar GmbH, Graz, Austria). For these measurements an adjustable gap cell, equipped with Ag/AgCl electrodes, was used. A measuring channel was built between two spin-coated silicon wafers, fixed between two electrodes. The measuring fluid (0.001 mol/L KCl solution) was streamed with varying pressure through this channel. The pH-dependent measurements were started at least 30 min after filling the cell at neutral pH; the pH value was altered stepwise by adding HCl solution or KOH solution, respectively. From the slope of streaming potential *vs.* pressure difference in the cell the zeta potential was calculated for each pressure ramp according to the Smoluchowski equation.[25, 26]

Ellipsometry measurements

Ellipsometry measurements were carried out using a Woollam M2000-UI spectroscopic ellipsometer (J.A. Woollam Co. Inc., Lincoln, USA). For in-air measurements, a wavelength range of 245-1690 nm was used, and measurements were obtained using incident angles of 60, 65, 70 and 75°. The data was processed using completeEASE software (J.A. Woollam Co. Inc.), and a box model with sharp interfaces for the polymer film on a native SiO_2/Si substrate was applied. The optical dispersions for SiO_2 and Si were taken from the database. The refractive index of the polymer film was modelled by a Cauchy dispersion $n(\lambda)=A+B/\lambda^2$. For polymer film thickness values smaller than 10 nm, fixed values of A = 1.520 and B = 0.006 were used for the refractive index (*n*) unless indicated.

PBS solution (pH 7.4, 0.01 mol dm^{-3}) was obtained by dissolving one PBS tablet in 200 mL deionised water. A 0.01 mol dm^{-3} solution of PBS contains 0.01 mol dm^{-3} phosphate buffer, 0.0027 mol dm^{-3} potassium chloride and 0.137 mol dm^{-3} sodium chloride.

Sodium phosphate buffer (pH 7.4, 0.001 mol dm^{-3}) was obtained by dissolving 0.109 g of sodium phosphate dibasic and 0.031 g of sodium phosphate monobasic in 1 L deionised water.

In-situ ellipsometry measurements were carried out at one angle of incidence at 68° using a 3 mL volume glass cuvette (quartz glass, fixed angle of cuvette sides at 68°, TSL Spectrosil, Hellma Analytics). All measurements were taken at room temperature. Dry measurements were taken with the coated wafer outside and inside the cuvette to correct for window effects, and the wafer was secured with a PTFE support. PBS buffer solution (pH 7.4, 0.01 mol dm^{-3}) was then added and the degree of swelling measured at regular time intervals (~18 s). When the film thickness value had become stable, at least 3 further measurements were recorded at different points on the film, and an average degree of swelling was modelled for a wavelength range of 370-900 nm.

Antibody adhesion measurements were carried out using a 1.3 mL glass cuvette with walls at 70° angles (Hellma Analytics, Jena, Germany). Dry measurements were taken with the coated wafer outside and inside the cuvette to correct for window effects, and the wafer was secured with a PTFE support. 1.3 mL sodium phosphate buffer solution at (pH 7.4, 0.001 mol dm^{-3}) was then added and measurements were recorded every ~45 s. When the thickness had become stable, 0.2 mL of buffer solution was removed using a syringe. 100 µL of a solution of anti-aflatoxin antibody (1 mg mL^{-1} in 0.001 mol dm^{-3} NaPB) was then introduced and the cell refilled with buffer solution to give a total antibody concentration of 0.08 mg mL^{-1}. Measurements of film thickness were recorded again, every ~45 s until the value became stable, and a single further measurement was taken with a wavelength range of 370-900 nm. 0.1 mL aliquots of antibody solution were then removed and replaced with buffer solution until the antibody concentration was reduced to 0.04 mg mL^{-1} and measurements were then recorded every 45 s until a stable value was reached. A final measurement was taken with a wavelength range of 370-900 nm.

Adsorption measurements using a quartz-crystal-microbalance (QCM-D)

Antibody adsorption measurements were carried out using a Q-Sense E4 flow quartz-crystal-microbalance with dissipation monitor (QCM-D , Biolin Scientific, Gothenburg, Sweden). Three SiO_2-coated, gold-plated quartz crystal electrodes were spin-coated with the copolymer followed by vacuum drying. Afterwards, the polymer-coated electrodes were mounted in the flow cell, and buffer solution (0.001 mol dm^{-3} sodium phosphate buffer, pH = 7.4) was passed through the cells at a flow rate of 0.1 mL/min until a stable baseline (frequency) was observed. The solution was then switched to a 0.025 mol dm^{-3} solution of an anti-aflatoxin antibody in the previously used buffer solution and passed through the cells until a plateau of the frequency was obtained. The solution was then switched back to buffer solution (to check for possible

Table 1. Polymerisation conditions and results for statistical copolymers prepared by free radical polymerisation in DMF at 70 °C with AIBN as initiator. The monomers HEMA (H), GMA (G), DMA (D) and initial monomer composition are indicated in the name of the polymer.

Polymer	t / h	Copolymer Composition	RM[a] Composition	Monomer conversion / %	M_n / g mol^{-1}	Đ
D-100	21	-	-	<10	-	-
H-100	21	-	-	94	17250	2.7
HD-90/10	21	92/8	45/55	95	13650	3.2
HD-80/20	21	84/16	24/76	93	10000	4.4
HD-70/30	21	75/25	34/66	84	3050	14.3
HD-61/39	21	71/29	16/84	81	3500	11.8
HD-50/50	21	59/41	5/95	83	17750	3.3
HG-89/11	18.5	78/22	89/11	83	133500	4.3
HGD-80/10/10	15	83/12/6	71/7/22	75	43400	3.2

a) Residual monomer composition.

desorption under this rinsing condition) and the whole process was repeated several times. After each measurement, the cell was washed with 0.1 mol dm^{-3} HCl and Millipore water before air was pumped into the system. Data was processed using the QSense Dfind software (Biolin Scientific, Sweden) using the Sauerbrey model.[27]

Results and Discussion

Polymer synthesis

A series of homo- and copolymers have been synthesised using free radical polymerisation with a view to investigate and establish the role that each monomer plays in the desired functional terpolymer (Scheme 1), particularly the effect of the catechol group in DMA (D). HEMA (H) was included to enhance hydrophilicity and biocompatibility, and GMA (G) to provide reactive sites for antibody immobilisation.

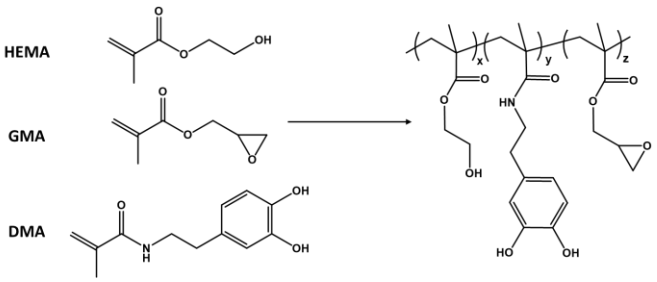

Scheme 1. Molecular structure of DMA/GMA/HEMA monomers and terpolymer.

Effect of DMA on properties of HEMA/DMA copolymers

Homopolymerisation of DMA resulted in a polymer obtained in low yield, which quickly turned brown and became insoluble in the presence of oxygen (D-100, Table 1). FR homopolymerisation of DMA has been reported by a limited number of other groups but has been generally overlooked due to potential for crosslinking, which may occur *via* coupling reactions between catechol-functionalised side chains by oxidation to the highly reactive quinone form.[28-30] It has been well-established in the literature that the catechol functional group is able to scavenge radicals via its quinone form by the donation of a hydrogen atom to a free radical.[31] Our result strongly supported the suggestion that crosslinking of poly(DMA) during FR polymerisation occurs readily.

The effect of DMA on copolymerisation with HEMA was explored by the synthesis of a series of copolymers using DMA molar fractions from 10 mol% to 50 mol% (see Table 1). In contrast to DMA homopolymerisation, high yields were obtained from copolymerisation with HEMA. The number-averaged molecular weight M_n for the HEMA/DMA copolymers ranged from 3050 – 17750 g mol^{-1}. A HEMA homopolymer (H-100) was synthesised as a control, yielding a higher M_n than the majority of HEMA/DMA copolymers (M_n = 17250 g mol^{-1} and Đ = 2.67). For the HEMA/DMA copolymers with DMA molar fractions < 40%, M_n generally decreased, and dispersity Đ increased with increasing DMA molar fraction, whilst the weight-averaged molecular weight M_w remained relatively constant between 40000 and 44000 g mol^{-1}. We suggest the dispersity trend is due to chain transfer to the catechol monomer, leading to the formation of short-chain species. This is similar to the observation of Kamperman *et al.*, who attributed reduced M_n with increasing DMA content to chain termination from radical scavenging.[30] A high chain-transfer constant for catechol-containing monomers has been previously predicted,[32] and chain-transfer leading to reduced molecular weights has been observed during the polymerisation of monomers with a mercaptan-functionalised side chain.[33] In our case, when the molar fraction of DMA was increased to >40%, M_n and M_w increased dramatically, suggesting catechol coupling (crosslinking) became dominant over chain transfer.

The molecular weight and dispersity trends here are in general agreement with two previously reported poly(HEMA-co-DMA) syntheses in which the effect of the catechol group was not discussed.[34, 35] The data obtained in the current study indicates that the effect of the catechol functional group on the molecular weight becomes greater as the molar fraction of DMA was increased. It is clear that compositional drift occurs, as each copolymer contained a smaller molar fraction of DMA than the initial monomer feed (Table 1). Furthermore, the residual (unreacted) monomer detected in the final sample of each reaction contained a greater proportion of DMA than the feed – strongly indicating the preferential incorporation of HEMA. The molar ratio of DMA in the initial monomer feed to the molar DMA ratio in

copolymer was 0.75 – 0.81, indicating a similar degree of compositional drift in each case and suggesting the compositional drift is not primarily due to radical scavenging. This finding can be rationalised by considering the recently reported reactivity ratios for a similar system in which acetonide-protected DMA (ADMA) was copolymerised with methyl methacrylate (MMA) (r_{MMA}= 2.21, r_{ADMA}= 0.17).[36] The strong preferential incorporation of the methyl methacrylate monomer over the methacrylamide was largely attributed to the relative reactivity of the polymerisable groups, which would also apply to the current work.

Effect of GMA on terpolymers

A terpolymer was also synthesised comprising DMA and HEMA with GMA, to introduce reactive side-chains into the polymer. The final composition of HGD-80/10/10 again indicated the preferential incorporation of methacrylate monomers, with final DMA content of 6%. A control polymer without DMA, HG-89/11, was also synthesised. The final composition of HG-89/11 was 78/22, indicating GMA was preferentially incorporated into the copolymer. The slight preference towards GMA incorporation is supported by a previous report, which indicated the reactivity ratios of HEMA and GMA at 60 °C in DMF were r_{HEMA} = 0.74, r_{GMA} = 1.00.[37]

Spin Coating of HEMA-containing copolymers

A series of copolymers, all containing molar fractions of at least 78 mol% HEMA, and ~20 mol% comonomer were spin-coated onto silicon wafer with the aim of obtaining uniform thin films. AFM was used to assess the nanometre-scale topography (roughness) of the films, whilst film thickness was measured by ellipsometry. All of the copolymers included in the study were soluble in methanol up to at least 2.0 wt.-% (w/v) concentration. HGD-80/10/10, HD-90/10 and HG-89/11 were spin-coated onto silicon wafer substrates using copolymer solution concentrations of between 0.5 wt.-% and 2.0 wt.-% (w/v), obtaining films between 26 and 165 nm thick. In some cases, it was observed that films contained defects – striations or porous structures. This was attributed to the highly volatile solvent and potentially premature precipitation of the copolymers from methanol. A full list of the samples coated from methanol can be found in Tables SI1 – SI3 in the supplementary information. Roughness values (R_a) of 0.3 nm (for HD-90/10 and HG-89/11), and 2 nm up to 25 nm (for HGD HGD-80/10/10) were measured by AFM, allowing the conclusion that most of the films were sufficiently smooth for further analysis.

Analysis of spin-coated polymer films

The spin-coated films of HGD-80/10/10, HD-90/10 and HG-89/11 were investigated by several techniques to determine their suitability for use in biosensing applications and to determine the relationship between surface properties and structure (composition and molar mass) of each copolymer, particularly the content of catechol and epoxide functional groups.

ADSA-P captive bubble contact angle

Contact angle measurements of selected copolymer films were used to study the wettability of the copolymer layers by water. For biosensing applications, the polymer films should be hydrophilic to enable interaction with analytes dissolved in aqueous solvent. Since ellipsometry revealed significant swelling of the polymers, as shown later in the discussion, contact angles of the water-swollen polymer layers were studied in water by an inverse technique, the ADSA-P captive bubble method.[23] In contrast to the sessile drop technique, it determines advancing (θ_a) and receding (θ_r) angles of the liquid surrounding an air bubble positioned under the swollen polymer layer, while the bubble volume is increased and decreased, respectively. To ensure full swelling, each film was immersed in the water for at least 30 minutes. Table 2 summarizes the advancing and receding contact angles of the water-swollen copolymer films HGD-80/10/10, HD-90/10 and HG-89/11, spin-coated on silicon wafer (1000 rpm, 400 rpm s^{-1}, 2% (w/v) solution in methanol).

Table 2. Water-contact angles of copolymer films obtained by ADSA-P captive bubble measurements.

Polymer	θ_a/°	θ_r/°	$\theta_a - \theta_r$ /°
HGD-80/10/10	65	21	44
HD-90/10	65	18	47
HG-89/11	76	13	63

The films showed no sign of delamination during the testing, indicating they were adhered well to the surface of the substrate. The time-dependent measurement of contact angle, bubble radius and bubble volume revealed smooth bubble expansion on the swollen polymer surfaces (see Figure SI-1 in the supporting information).

HGD-80/10/10 and HD-90/10 exhibited an advancing contact angle of 65° suggesting they are moderately hydrophilic. The receding contact angle of both films was, however, significantly smaller, in the order of about 20°. Thus, the contact angle hysteresis, *i.e.* the difference between advancing and receding contact angle, was relatively high. HG-89/11 showed a slightly higher advancing contact angle than the other copolymer films but can still be regarded slightly hydrophilic. The contact angle hysteresis was even more pronounced. In the literature, different explanations are discussed for the occurrence of contact angle hysteresis including roughness, chemical inhomogeneity of the film, or reorientation of (co)polymer molecules in the swollen layer near the three-phase contact line. In the case of the polymers studied, the maximum roughness R_a measured by AFM on some of the samples ($R_a \leq 25$ nm, see Table SI-4) for each of the relevant copolymers was much lower than the threshold value for feature depth to affect hysteresis, thought to be at around 100 nm.[38] In the swollen state, the roughness is assumed to be reduced further, even in the case of the porous films of HGD-80/10/10. In the swollen copolymer state, chain mobility is increased, and consequently surface pore size may be reduced or the pores may disappear entirely.[39] Therefore, the contact angle hysteresis is attributed to a change in the polymer conformation near the three-phase contact line, preventing any motion of the contact line while the polymer equilibrates to its lowest energy conformation in the new medium.[40]

The water contact angles of the three copolymers did not differ significantly. GMA is a monomer without polar groups resulting in rather hydrophobic films, while HEMA and DMA contain polar

hydroxyl groups. Therefore, the slightly higher advancing contact angle of HG-89/11 might result from its GMA content. The contact angle of HGD-80/10/10 seems unaffected by the GMA moieties.

Streaming potential measurements

Streaming potential measurements were used to determine the zeta potential (ζ) of the polymer films in 1 mmol L^{-1} KCl solution, as a function of the pH value. The zeta potential is a measure of the surface charge of a solid surface in contact with an aqueous solution. It may influence the interaction between the polymer film and biomolecules which usually also carry charged sites.[41] On the other hand, the behaviour of the zeta potential as function of the pH value gives valuable information on dissociable groups at solid surfaces.[25, 26]

Figure 1 presents the zeta potential curves of two copolymers, HD-90/10 and HGD-80/10/10, in comparison with the homopolymers poly(HEMA), poly(DMA) and poly(GMA), and a blank silicon wafer. Reliable results could not be obtained for HG-89/11, suggesting the film was unstable under the measurement conditions. All polymers exhibited a transition from positive to negative zeta potential in the acidic pH range. The zero crossing of the zeta potential, the isoelectric point (IEP), is an important parameter for the interpretation of zeta potential curves. An IEP at pH 2.5-3, as shown by all polymers except poly(GMA), indicates the presence of dissociable acidic groups. This can be explained by the hydroxyl groups in HEMA and DMA units which dissociate to form anions. On the contrary, poly(GMA) had the IEP near pH 4, a feature typical for uncharged polymers. At pH values above the IEP, negative ζ values were obtained, caused by the preferable adsorption of anions (OH^-) from the solution, a commonly observed phenomenon, even in non-ionic polymers such as poly(MMA).[42] The zeta potential curves of HGD-80/10/10 and HD-90/10 are very close to those of poly(HEMA) and poly(DMA). This suggests that the GMA in HGD-80/10/10 had no significant effect on ζ. In hydrogels with functional groups that dissociate to form anions (*e.g.* carboxylic acid or hydroxyl groups), the zeta potential can become less negative due to pH-influenced swelling.[43] The weak differences of the plateau values of the zeta potential in the alkaline range may be caused by a slightly different water-uptake of the copolymer layers.

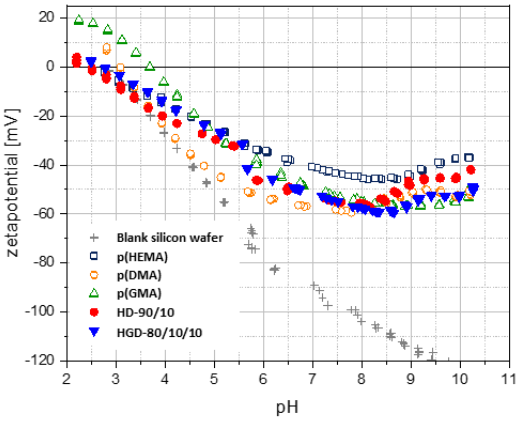

Figure 1. Zeta potential of the spin-coated films of HGD-80/10/10 and HD-90/10 compared to the homopolymers and a blank silicon wafer.

In-situ ellipsometry

To further investigate the degree of swelling of the copolymer films, *in-situ* ellipsometry was used to monitor swelling of spin-coated polymer films in an aqueous buffer solution at pH 7.4. Hydrogel swelling has been associated with increased protein adsorption to the polymer layer.[44] The film structure and resistance of the copolymer film to dissolution (due to surface adhesion of the copolymer and intermolecular interactions) can be also inferred from the *in-situ* measurements and are critical for the intended application. The swelling of glassy polymers generally can be described by either Fickian (diffusion-limited) dynamics or Case II (non-diffusion limited) dynamics.[45] This can be determined using *in-situ* ellipsometry by monitoring the change in film thickness, *h*, and refractive index, *n*, over time.

The swelling dynamics of several HEMA-containing homo- and copolymers have been reported.[19, 46] Cross-linked poly(HEMA) hydrogels undergo swelling in water with film thickness increases of up to 55%. An increase in cross-link density results in a decrease in swelling. However, it was reported that in poly(HEMA) films deposited by chemical vapour deposition of distilled monomer, the homopolymer fully desorbed in water after 15 minutes.[40] In the work described here, the copolymer films studied using contact angle and ellipsometry measurements did not noticeably dissolve or delaminate.

Figure 2 shows the *in-situ* ellipsometry measurements of the copolymers. Film thickness and normalised refractive index (n_{norm}) are plotted against the time *t*. n_{norm} was calculated using Equation 1:

$$\boldsymbol{n_{norm} = \frac{n_{swollen} - n_{buffer}}{n_{dry} - n_{buffer}}} \qquad \textbf{1}$$

where $n_{swollen}$, n_{dry}, n_{buffer} are the refractive indices for the swollen copolymer, the dry copolymer and the buffer solution respectively (at λ = 633 nm).[45] n_{norm} is used as a comparative measure of the optical properties of the copolymer film. A value of 1 would indicate the refractive index of the film was unchanged upon immersion in solvent (*i.e.* no swelling or dissolution), while a n_{norm} approaching 0 would indicate the refractive index of the immersed film became identical to that of the solvent. A value greater than 1 may occur if the dry copolymer film contains a significant volume of air voids, which are filled with solvent in the swollen film.

Film thicknesses obtained from the dry film (h_{dry}) are shown by a blue dashed line in Figure 2. A swelling factor (SF) was also calculated using Equation 2 to compare the relative increase in the film thickness. SF values are shown in Table 3. Full data can be found in Table SI-5. It should be noted that over extended time periods (days/weeks), the copolymers may continue to slowly relax or diffuse to a final equilibrium film structure,[45] although such timescales were not considered relevant to the current application.

$$\boldsymbol{SF = \frac{h_{final}}{h_{dry}}} \qquad \textbf{2}$$

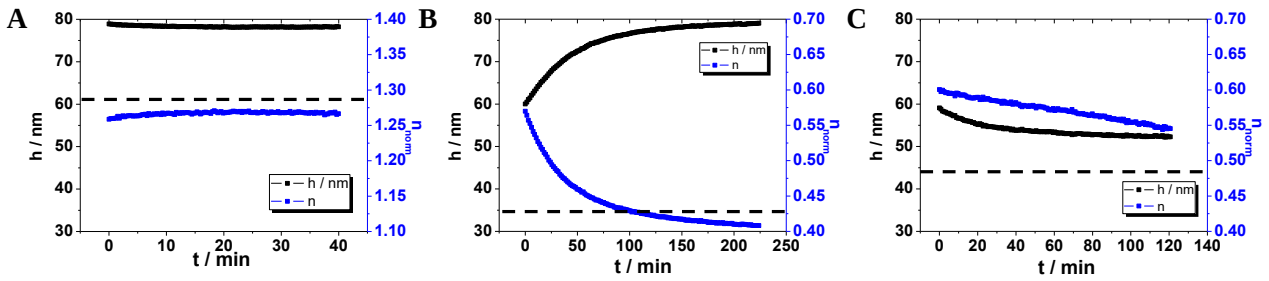

Figure 2. Film thickness (h, black) and normalised refractive index (n_{norm}, blue) vs time for *in-situ* ellipsometry measurements of A) HGD-80/10/10, B) HD-90/10 and C) HG-89/11 . Black dashed line indicated dry film thickness.

Initial swelling of HGD-80/10/10 (Figure 2A) took place rapidly (before the first *in-situ* measurement). In this time the copolymer film had swollen from an initial dry thickness of 60 nm to 79 nm. Rapid swelling, often followed by a slower change in film thickness due to chain relaxation, is commonly observed and is characteristic of the solvent filling free-volume in an amorphous copolymer (*i.e.* rapid entry of solvent into regions not occupied by the copolymer matrix).[44, 45, 47]

Table 3. Properties of *in-situ* polymer swelling measurements.

Polymer	h_{dry} / nm	n_{dry}	SF	Ω
HGD-80/10/10	61	1.42	1.28	0.2
HD-90/10	36	1.51	2.19	5.6
HG-89/11	44	1.50	1.34	19.7

For HGD-80/10/10, after the initial rapid swelling, film thickness decreased very slightly (-0.7 nm) over the 40 min measurement period, and n_{norm} increased concomitantly, with a final swelling factor of 1.28 (Figure 2A). The very small reduction in film thickness suggested slight relaxation of the copolymer chains to the equilibrium conformation following the rapid swelling.[48] This behaviour is characteristic of Case II swelling with limited overshoot dynamics.[45] The high equilibrium value of n_{norm} indicated the presence of a significant volume of air in the dry copolymer film (n_{norm} = 1.27, note the different scale for n_{norm} and *t* in comparison with Figures 2B and C). It can therefore be implied that porous films were produced when HGD-80/10/10 were spin-coated from methanol and the film thickness increase was reduced by polymer swelling into pores. The porosity of the film would also enable the solvent to rapidly pass through the entire film via the air voids.

In the case of HD-90/10, after the initial fast swelling from 36 to 60 nm, the copolymer film continued to swell, with a synchronous decrease in n_{norm} suggesting Fickian (diffusion-controlled) swelling dynamics (Figure 2B). The diffusion-controlled swelling dynamics, low value of n_{norm} (0.40) and swelling factor of 2.19 indicate that significant swelling of the film arises from solvent diffusion in the absence of air voids. The increase in film thickness when plotted against $t^{0.5}$ does not yield a perfectly linear curve, indicating simultaneous solvent diffusion and relaxation processes were occurring.[48]

For HG-89/11, a similar initial rapid increase in film thickness was observed (from 44 nm to 59 nm, Figure 2C). The swelling factor was 1.34, which was similar to HGD-80/10/10, suggesting significant desorption of the polymer in the absence of DMA. The *in-situ* ellipsometry profile of HG-89/11 was dramatically different from the previously described copolymers. Both film thickness and refractive index decreased with time. This trend strongly suggested copolymer dissolution/desorption.[45] It is therefore proposed that the absence of DMA reduced the surface adhesion and intermolecular cohesion in the polymer. This finding is consistent with the contact angle analysis, in which HG-89/11 has the largest hysteresis, assigned to increased surface mobility of the copolymer chains due to the absence of DMA.

Polymer dissolution or desorption would indicate undesirably poor film stability; however, which cannot be confirmed by film thickness alone, as both swelling and dissolution can influence the film thickness. A dissolution factor, Ω (see 3), was therefore calculated using the de Feijter equation to decouple the two effects by calculating the surface mass density of the deposited film *i.e.* the amount of material in a film per surface area (see Supporting Information).[49] Ω measures the percentage of copolymer lost *via* dissolution between the initial and final measurements *e.g.* a Ω of 5% indicates that in the period from the first measurement after buffer was added, 5% of the mass was lost to dissolution. Due to the change of ambient environment (change from air to buffer solution), this calculation was not applied to the dry film, so the period between adding the buffer and the first ellipsometry measurement is not considered. Significant swelling occurred in this period, so the full extent of dissolution may not be reflected. The average time between filling the cell with buffer and beginning *in-situ* measurements was around 1 minute. A value of n_{amb} = 1.3329 was used for the buffer solution (0.01 mol dm^{-1} PBS buffer, measured using a refractometer).

For HGD-80/10/10, Ω was 0.2%, indicating virtually no copolymer dissolved after the initial swelling period. The limited dissolution over a period of 40 minutes suggests the remaining copolymer film was strongly adsorbed and stable. Similarly, for HD-90/10 the value for Ω was 5.4% indicating limited dissolution after the initial swelling. This result suggested the DMA in HD-90/10 was providing strong adhesion to the surface of the substrate and cohesive interactions with other polymers, as also indicated by the contact angle measurements. However, adhesion was slightly poorer than for HGD-80/10/10. This could be due to the relatively low molecular

weight, which may allow poorly bound chains to dissolve more rapidly. In contrast, the indicated significant dissolution of HG-89/11 was confirmed by a large Ω of 19.7%. This was attributed to a lack of DMA-induced adhesive and cohesive interactions. This result highlights the crucial role of DMA in providing adhesion to the substrate and cohesion in the copolymer film. Overall, the ellipsometry results demonstrated the significant influence of the DMA on the polymer film behaviour.

Coating of antibodies on a film of HGD-80/10/10

The copolymers in this study were designed and synthesised with a view to immobilisation of an antibody onto a copolymer film for use in biosensing devices. To explore this possibility, an attempt was made to immobilise anti-aflatoxin M1 antibody from an aqueous buffer solution onto a film of HGD-80/10/10, *via* chemical reaction between the epoxide groups of GMA and primary amine or thiol-protein residues. The success of antibody immobilisation was monitored using two complementary methods: *in-situ* ellipsometry and QCM-D. HGD-80/10/10 comprised GMA for covalent immobilisation of biomolecules,[50] and DMA for adhesion to various substrates, as indicated by the very limited dissolution of HGD-80/10/10 and HD-90/10 in buffer solution.

Anti-aflatoxin M1, used in this study, is an IgG type antibody. IgG antibodies are Y-shaped proteins with dimensions of around 14.5 x 8.5 x 4 nm,[51] and molecular weight in the region of 150000 – 160000 g mol^{-1}.[52] The surface mass density of a layer of immobilised antibody, Γ, can be calculated using the film thickness and refractive index values obtained from ellipsometry measurements.[49]

Characterisation of antibody immobilisation using in-situ ellipsometry

In-situ ellipsometry was used to monitor the immobilisation of anti-aflatoxin M1 antibody to the surface of a silicon wafer, spin-coated with HGD-80/10/10 (0.75% (w/v) from methanol, 4000 rpm, 600 rpm s^{-1}). Sodium phosphate buffer (NaPB, 0.001 mol dm^{-3}) was used for the measurements. A 0.08 mg mL^{-1} antibody solution concentration was used for the immobilisation experiments. The refractive index of the NaPB was accurately determined using a refractometer (n(633 nm) = 1.3315).

The spin-coated silicon wafer sample (dry film thickness 34 nm) was immobilised in a trapezoidal cuvette and allowed to swell in NaPB (0.001 mol dm^{-3}). The film was judged to have reached an equilibrium state when the values for film thickness and *n*(633 nm) showed minimal further change at 46 nm and 1.48 respectively (SF = 1.35). The pure buffer solution was then replaced with a solution of antibody (final concentration 0.08 mg mL^{-1}) in NaPB (0.001 mol dm^{-3}). The polymer film thickness increased by 7 nm compared to the pre-swollen film to 52.9 ± 0.1 nm (average for measurements after 35 min) (**Error! Reference source not found.**3A). Several previous reports suggest that the thickness of an IgG antibody monolayer is in the region of 4 – 8 nm.[51, 53, 54] Therefore, The observed thickness increase is consistent with a monolayer antibody coating, but note that the measurement cannot resolve the depth distribution of antibodies on or within the film. Very limited antibody desorption was observed when the

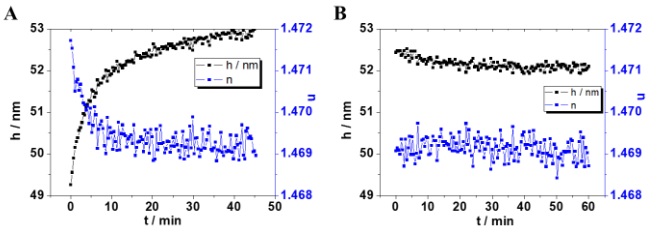

Figure 3. *In-situ* ellipsometry measurements of HGD-80/10/10 for immobilisation of antibody in 0.001 mol dm^{-3} phosphate buffer solution. A) Adsorption from 0.08 mg mL^{-1} antibody. B) Antibody concentration reduced to 0.04 mg mL^{-1}.

concentration of the antibody solution was reduced to 0.04 mg mL^{-1} (final thickness 52.1 ± 0.1 nm, **Error! Reference source not found.**3B), indicating permanent antibody immobilisation in the buffer solution used. The mass of coated antibody can be calculated using a modified form of the De Feijter equation (see Equation 3) to build a two-layer model of the deposition as outlined by Bittrich *et al.*[55]:

$$\Gamma_{ab} = d_{swell} \cdot \frac{n_{ab} - n_{swell}}{(dn/dc)_{ab}} + d_{add} \cdot \frac{n_{ab} - n_{amb}}{(dn/dc)_{ab}} \qquad 3$$

where Γ_{ab} is the absorbed amount of the immobilised layer of antibody, in mg m^{-2}, d_{swell} and d_{add} refer to the thickness of the swollen copolymer and the additional layer, n_{ab} ,n_{swell} and n_{amb} are the refractive indices of the film after antibody adhesion, the swollen copolymer and the ambient solution respectively. A *dn/dc* of 0.188 was used for the antibody.[52] Using film thickness and *n*(633 nm) values collected after the antibody concentration had been reduced (52 nm and 1.469 respectively), a Γ_{ab} value of 3.5 mg m^{-2} was calculated. The Γ_{ab} value was similar to literature values (4 – 4.6 mg m^{-2}) for monolayers of anti-aflatoxin M1 antibody on a colloidal latex particle,[56] supporting the claim of successful immobilisation of an amount equivalent to an antibody monolayer.

Characterisation of antibody binding using QCM-D

The deposition of anti-aflatoxin antibody on a film of HGD-80/10/10 was also investigated using QCM-D with the intention to covalently bind the antibodies to the film via the epoxide side chains. Frequency shift (*Δf*) and dissipation shift (*ΔD*) data were obtained and the multiple harmonic overtone frequencies contributed to the modelling of the data. Frequency shifts of -40 to -60 Hz and dissipation shifts of 2×10^{-6} to 9×10^{-6} were obtained. The antibody film thickness was calculated using the Sauerbrey equation, with an estimated ρ_f value of 1 g cm^{-3} (Figure 4).[27, 57] The criterion for film rigidity ($\Delta D_n/(\Delta f_n/n) << 0.4 \times 10^{-6}$ Hz^{-1}) was met by overtones 3 - 7, justifying the use of the Sauerbrey equation for these films.[58]

Passage of anti-aflatoxin antibody (0.025 mg mL^{-1}) in NaPB (0.001 mol dm^{-3}) was accompanied by a sharp increase in the calculated film thickness ("Ab(1)" and "Ab(2)" on Figure 4). This strongly indicated an increase of mass on the electrode, suggesting immobilisation of the antibody on the electrode surface.[59]

Flushing with buffer solution (Buffer(1) and Buffer (2)), resulted in only a small reduction in film thickness (~-0.5 nm). The overall film

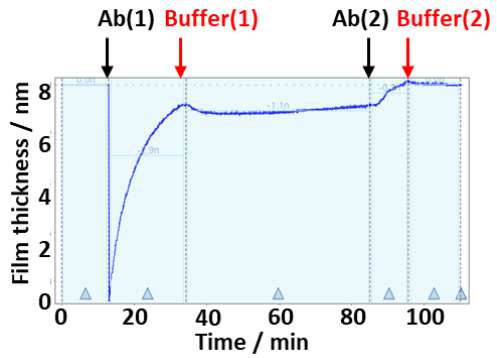

thickness increase of 8 nm (Figure 4) correlated well with the results

Figure 4. QCM data for immobilisation of 0.025 mg mL^{-1} antibody for aflatoxin M1 to a film of HGD-80/10/10. Film thickness vs time, two immersion/rinse cycles.

of the *in-situ* ellipsometry, where a thickness increase of 7 nm was detected. This may be a monolayer coating, although the film thickness could also be affected by antibody penetration into the swollen film.

The combined data from QCM and ellipsometry therefore appeared to provide consistent evidence that a layer of anti-aflatoxin antibody was immobilised on the film of HGD-80/10/10. HGD-80/10/10 may therefore be an appropriate candidate for use in biosensing applications. Further research is required to extend this preliminary study to investigate the binding mechanism of the antibody to the film and determine the activity and sensitivity of the antibodies towards aflatoxin.

Conclusions

A novel terpolymer comprising HEMA, GMA and DMA was synthesised, characterised and demonstrated to be suitable for immobilising antibodies on a surface for biosensing applications. It was demonstrated that the catechol functional group has a direct effect on the dispersity and molecular weight of the copolymer, attributed to chain transfer to monomer, which increases as the proportion of catechol containing monomers in the feed is increased. We show that the inclusion of three key moieties that enable tuneable hydrophilicity, antibody binding and substrate binding are flexibly incorporated into a single polymer.

Streaming potential and contact angle measurements demonstrated the films containing DMA were hydrophilic and relatively stable. The significant contact angle hysteresis suggested chain mobility around the three-phase contact line. Clear hydrogel swelling was measured by in-situ ellipsometry. The significant polymer desorption observed in the absence of DMA highlighted the crucial role played by the catechol group in providing surface adhesion and cohesion to the polymer. An IgG antibody could be immobilised on the surface of a film of the terpolymer HGD-80/10/10. This was demonstrated by an increase of film thickness measured by both ellipsometry and QCM. The results consistently showed that the antibody binding corresponded closely to a surface monolayer, which would be an ideal configuration for sensor applications.

Acknowledgements

The UK Engineering and Physical Sciences Research Council (EPSRC) is acknowledged for financial support of the Centre for Doctoral Training in Soft Matter and Functional Interfaces (Grant Number EP/L015536/1). Andreas Janke (IPF Dresden) is acknowledged for AFM measurements and calculation of roughness. Susanne Stehl (IPF Dresden) is acknowledged for technical support with QCM-D measurements.

References

[1] A. Karczmarczyk, M. Dubiak-Szepietowska, M. Vorobii, C. Rodriguez-Emmenegger, J. Dostalek, K.H. Feller, Sensitive and rapid detection of aflatoxin M1 in milk utilizing enhanced SPR and p(HEMA) brushes, Biosens Bioelectron 81 (2016) 159-165.
[2] Commission Regulation (EC) No 1881/2006, European Commission, 2006.
[3] L.K. Sorensen, T.H. Elbaek, Determination of mycotoxins in bovine milk by liquid chromatography tandem mass spectrometry, Journal of Chromatography, B: Analytical Technologies in the Biomedical and Life Sciences 820(2) (2005) 183-96.
[4] H. Wang, X.J. Zhou, Y.Q. Liu, H.M. Yang, Q.L. Guo, Simultaneous determination of chloramphenicol and aflatoxin M1 residues in milk by triple quadrupole liquid chromatography-tandem mass spectrometry, J Agric Food Chem 59(8) (2011) 3532-8.
[5] N.W. Turner, H. Bramhmbhatt, M. Szabo-Vezse, A. Poma, R. Coker, S.A. Piletsky, Analytical methods for determination of mycotoxins: An update (2009-2014), Anal Chim Acta 901 (2015) 12-33.
[6] W. Hu, X. Li, G. He, Z. Zhang, X. Zheng, P. Li, C.M. Li, Sensitive competitive immunoassay of multiple mycotoxins with non-fouling antigen microarray, Biosens Bioelectron 50 (2013) 338-44.
[7] H. Lee, J. Rho, P.B. Messersmith, Facile Conjugation of Biomolecules onto Surfaces via Mussel Adhesive Protein Inspired Coatings, Adv Mater 21(4) (2009) 431-434.
[8] H. Lee, S.M. Dellatore, W.M. Miller, P.B. Messersmith, Mussel-inspired surface chemistry for multifunctional coatings, Science 318(5849) (2007) 426-430.
[9] J.H. Ryu, P.B. Messersmith, H. Lee, Polydopamine Surface Chemistry: A Decade of Discovery, ACS Appl Mater Interfaces 10(9) (2018) 7523-7540.
[10] H. Lee, B.P. Lee, P.B. Messersmith, A reversible wet/dry adhesive inspired by mussels and geckos, Nature 448(7151) (2007) 338-41.
[11] N. Patil, C. Falentin-Daudré, C. Jérôme, C. Detrembleur, Mussel-inspired protein-repelling ambivalent block copolymers: controlled synthesis and characterization, Polym. Chem. 6(15) (2015) 2919-2933.
[12] A. GhavamiNejad, C.H. Park, C.S. Kim, In Situ Synthesis of Antimicrobial Silver Nanoparticles within Antifouling Zwitterionic Hydrogels by Catecholic Redox Chemistry for Wound Healing Application, Biomacromolecules 17(3) (2016) 1213-23.
[13] P. Glass, H. Chung, N.R. Washburn, M. Sitti, Enhanced reversible adhesion of dopamine methacrylamide-coated elastomer microfibrillar structures under wet conditions, Langmuir : the ACS journal of surfaces and colloids 25(12) (2009) 6607-12.
[14] N. Patil, C. Jérôme, C. Detrembleur, Recent advances in the synthesis of catechol-derived (bio)polymers for applications in energy storage and environment, Prog. Polym. Sci. 82 (2018) 34-91.
[15] E. Faure, C. Falentin-Daudré, C. Jérôme, J. Lyskawa, D. Fournier, P. Woisel, C. Detrembleur, Catechols as versatile platforms in polymer chemistry, Prog. Polym. Sci. 38(1) (2013) 236-270.

[16] F.J. Holly, Wettability of Hydrogels .1. Poly(2-hydroxyethyl methacrylate), Journal of Biomedical Materials Research 9(3) (1975) 315-326.
[17] L. Uzun, R. Say, A. Denizli, Porous poly(hydroxyethyl methacrylate) based monolith as a new adsorbent for affinity chromatography, React. Funct. Polym. 64(2) (2005) 93-102.
[18] C. Rodriguez-Emmenegger, O.A. Avramenko, E. Brynda, J. Skvor, A.B. Alles, Poly(HEMA) brushes emerging as a new platform for direct detection of food pathogen in milk samples, Biosens. Bioelectron. 26(11) (2011) 4545-51.
[19] S. Akgöl, G. Bayramoğlu, Y. Kacar, A. Denizli, M.Y. Arıca, Poly(hydroxyethyl methacrylate-co-glycidyl methacrylate) reactive membrane utilised for cholesterol oxidase immobilisation, Polymer International 51(12) (2002) 1316-1322.
[20] Z. Lei, J. Gao, X. Liu, D. Liu, Z. Wang, Poly(glycidyl methacrylate-co-2-hydroxyethyl methacrylate) Brushes as Peptide/Protein Microarray Substrate for Improving Protein Binding and Functionality, ACS Appl Mater Interfaces 8(16) (2016) 10174-82.
[21] X.W. Fan, L.J. Lin, J.L. Dalsin, P.B. Messersmith, Biomimetic Anchor for Surface-Initiated Polymerization from Metal Substrates, J. Am. Chem. Soc. 127 (2005) 15843-15847.
[22] J. Brandrup, E.H. Immergut, Polymer Handbook, 3rd ed., Wiley Interscience1989.
[23] K. Grundke, K. Poschel, A. Synytska, R. Frenzel, A. Drechsler, M. Nitschke, A.L. Cordeiro, P. Uhlmann, P.B. Welzel, Experimental studies of contact angle hysteresis phenomena on polymer surfaces - Toward the understanding and control of wettability for different applications, Adv Colloid Interface Sci 222 (2015) 350-76.
[24] A.W. Neumann, J.K. Spelt, Applied surface thermodynamics, CRC Press1996.
[25] R. Zimmermann, S. Dukhin, C. Werner, Electrokinetic measurements reveal interfacial charge at polymer films caused by simple electrolyte ions, The Journal of Physical Chemistry B 105(36) (2001) 8544-8549.
[26] H.J. Jacobasch, Characterisation of solid surfaces by electrokinetic measurements, Progress in Organic Coatings 17 (1989) 115-133.
[27] I. Reviakine, D. Johannsmann, R.P. Richter, Hearing what you cannot see and visualizing what you hear: interpreting quartz crystal microbalance data from solvated interfaces, Anal. Chem. 83(23) (2011) 8838-48.
[28] J. Wang, M.N. Tahir, M. Kappl, W. Tremel, N. Metz, M. Barz, P. Theato, H.-J. Butt, Influence of Binding-Site Density in Wet Bioadhesion, Adv. Mater. 20(20) (2008) 3872-3876.
[29] H.J. Meredith, J.J. Wilker, The Interplay of Modulus, Strength, and Ductility in Adhesive Design Using Biomimetic Polymer Chemistry, Adv. Funct. Mater. 25(31) (2015) 5057-5065.
[30] J. Yang, J. Keijsers, M. van Heek, A. Stuiver, M.A. Cohen Stuart, M. Kamperman, The effect of molecular composition and crosslinking on adhesion of a bio-inspired adhesive, Polym. Chem. 6(16) (2015) 3121-3130.
[31] M.S. Kharasch, F. Kawahara, W. Nudenberg, The Mechanism of Action of Inhibitors in Free Radical Initiated Polymerizations at Low Temperatures, Journal of Organic Chemistry 19(12) (1954) 1977-1990.
[32] Y.S. Choi, H. Kang, D.G. Kim, S.H. Cha, J.C. Lee, Mussel-inspired dopamine- and plant-based cardanol-containing polymer coatings for multifunctional filtration membranes, ACS Appl. Mater. Interfaces 6(23) (2014) 21297-307.
[33] L. Jiang, W.Y. Huang, X.Q. Xue, H.J. Yang, B.B. Jiang, D.L. Zhang, J.B. Fang, J.H. Chen, Y. Yang, G.Q. Zhai, L.Z. Kong, S.F. Wang, Radical Polymerization in the Presence of Chain Transfer Monomer: An Approach to Branched Vinyl Polymers, Macromolecules 45(10) (2012) 4092-4100.
[34] A.R. Sasikala, A. Ghavami Nejad, A.R. Unnithan, R.G. Thomas, M. Moon, Y.Y. Jeong, C.H. Park, C.S. Kim, A smart magnetic nanoplatform for synergistic anticancer therapy: manoeuvring mussel-inspired functional magnetic nanoparticles for pH responsive anticancer drug delivery and hyperthermia, Nanoscale 7(43) (2015) 18119-28.
[35] H.N. Nguyen, E.T. Nadres, B.G. Alamani, D.F. Rodrigues, Designing polymeric adhesives for antimicrobial materials: poly(ethylene imine) polymer, graphene, graphene oxide and molybdenum trioxide – a biomimetic approach, J. Mater. Chem. B 5(32) (2017) 6616-6628.
[36] N.A. Boulding, J.M. Millican, L.R. Hutchings, Understanding copolymerisation kinetics for the design of functional copolymers via free radical polymerisation, Polymer Chemistry 10(41) (2019) 5665-5675.
[37] D. Mohan, G. Radhakrishnan, S. Rajadurai, K.T. Joseph, Evaluation of Reactivity Ratio of Acrylate Copolymers by C-13-NMR, Journal of Polymer Science Part C-Polymer Letters 28(10) (1990) 307-314.
[38] C.W. Extrand, Y. Kumagai, An experimental study of contact angle hysteresis, J. Colloid Interface Sci. 191(2) (1997) 378-383.
[39] R. Zaleski, P. Krasucka, K. Skrzypiec, J. Goworek, Macro- and Nanoscopic Studies of Porous Polymer Swelling, Macromolecules 50(13) (2017) 5080-5089.
[40] K. Chan, K.K. Gleason, Initiated chemical vapor deposition of linear and cross-linked poly(2-hydroxyethyl methacrylate) for use as thin-film hydrogels, Langmuir 21(19) (2005) 8930-8939.
[41] C. Bellmanna, C. Klingerb, A. Opfermannc, F. Böhmea, H.-J.P. Adlerd, Evaluation of surface modification by electrokinetic measurements, Prog. Org. Coat. 44 (2002) 93-98.
[42] J. Lyklema, Surface charges and electrokinetic charges: Distinctions and juxtapositionings, Colloids Surf., A 376(1-3) (2011) 2-8.
[43] R. Zimmermann, D. Kuckling, M. Kaufmann, C. Werner, J.F.L. Duval, Electrokinetics of a Poly(N-isopropylacrylamid-co-carboxyacrylamid) Soft Thin Film: Evidence of Diffuse Segment Distribution in the Swollen State, Langmuir 26(23) (2010) 18169-18181.
[44] G. Guzman, S.M. Bhaway, T. Nugay, B.D. Vogt, M. Cakmak, Transport-Limited Adsorption of Plasma Proteins on Bimodal Amphiphilic Polymer Co-Networks: Real-Time Studies by Spectroscopic Ellipsometry, Langmuir 33(11) (2017) 2900-2910.
[45] E.J. Kappert, M.J.T. Raaijmakers, K. Tempelman, F.P. Cuperus, W. Ogieglo, N.E. Benes, Swelling of 9 polymers commonly employed for solvent-resistant nanofiltration membranes: A comprehensive dataset, J. Membr. Sci. 569 (2019) 177-199.
[46] L. Brannonpeppas, N.A. Peppas, Dynamic and Equilibrium Swelling Behavior of pH-sensitive Hydrogels Containing 2-Hydroxyethyl Methacrylate, Biomaterials 11(9) (1990) 635-644.
[47] D. Turnbull, M.H. Cohen, Free-volume Model of Amorphous Phase - Glass Transition, Journal of Chemical Physics 34(1) (1961) 120.
[48] Y. Tang, J.R. Lu, A.L. Lewis, T.A. Vick, P.W. Stratford, Swelling of zwitterionic polymer films characterized by spectroscopic ellipsometry, Macromolecules 34(25) (2001) 8768-8776.
[49] J.A. De Feijter, J. Benjamins, F.A. Veer, Ellipsometry as a Tool to Study the Adsorption Behavior of Synthetic and Bio Polymers at the Air Water Interface, Biopolymers 17(7) (1978) 1759-1772.
[50] G. Bayramoglu, S. Akgol, A. Bulut, A. Denizli, M.Y. Arica, Covalent immobilisation of invertase onto a reactive film composed of 2-hydroxyethyl methacrylate and glycidyl methacrylate:

properties and application in a continuous flow system, Biochemical Engineering Journal 14(2) (2003) 117-126.
[51] K.-B. Lee, S.-J. Park, C.A. Mirkin, J.C. Smith, M. Mrksich, Protein Nanoarrays Generated By Dip-Pen Nanolithography, Science 295 (2002) 1702-1705.
[52] C.G. Golander, E. Kiss, Protein Adsorption on Functionalized and Esca-characterized Polymer-films Studied by Ellipsometry, Journal of Colloid and Interface Science 121(1) (1988) 240-253.
[53] K. Wadu-Mesthrige, S. Xu, N.A. Amro, G.Y. Liu, Fabrication and imaging of nanometer-sized protein patterns, Langmuir 15(25) (1999) 8580-8583.
[54] M.E. BrowningKelley, K. WaduMesthrige, V. Hari, G.Y. Liu, Atomic force microscopic study of specific antigen/antibody binding, Langmuir 13(2) (1997) 343-350.
[55] E. Bittrich, P. Uhlmann, K.-J. Eichhorn, K. Hinrichs, D. Aulich, A. Furchner, Polymer Brushes, Hydrogels, Polyelectrolyte Multilayers: Stimuli-Responsivity and Control of Protein Adsorption, Ellipsometry of Functional Organic Surfaces and Films, Springer2014, pp. 79-105.
[56] A. Kondo, S. Uchimura, K. Higashitani, Immunological Agglutination Behavior of Latex Particles with Covalently Immobilized Antibodies, J. Ferment. Bioeng. 78(2) (1994) 164-169.
[57] S. Adam, M. Koenig, K.B. Rodenhausen, K.-J. Eichhorn, U. Oertel, M. Schubert, M. Stamm, P. Uhlmann, Quartz crystal microbalance with coupled spectroscopic ellipsometry-study of temperature-responsive polymer brush systems, Appl. Surf. Sci. 421 (2017) 843-851.
[58] E. Bittrich, F. Mele, A. Janke, F. Simon, K.-J. Eichhorn, B. Voit, D. Appelhans, Interactions of bioactive molecules with thin dendritic glycopolymer layers, Biointerphases 13(6) (2018) 06D405.
[59] F. Hook, M. Rodahl, P. Brzezinski, B. Kasemo, Energy dissipation kinetics for protein and antibody-antigen adsorption under shear oscillation on a quartz crystal microbalance, Langmuir 14(4) (1998) 729-734.